Organic Electronics 13 (2012) 985–991

Contents lists available at SciVerse ScienceDirect

Organic Electronics

journal homepage: www.elsevier.com/locate/orgel

Computational design of low singlet–triplet gap all-organic molecules for OLED application

Begoña Milián-Medina, Johannes Gierschner *

Madrid Institute for Advanced Studies, IMDEA Nanoscience, UAM, Modulo C-IX, Av. Tomás y Valiente 7, Campus Cantoblanco, 28049 Madrid, Spain

ARTICLE INFO

Article history:
Received 1 September 2011
Received in revised form 29 January 2012
Accepted 11 February 2012
Available online 5 March 2012

Keywords:
Organic light emitting diodes
Organic solar cells
Material design
Optical properties
External quantum efficiency
Singlet–triplet gaps

ABSTRACT

It was recently reported that external quantum efficiency in organic LEDs can be substantially enhanced when triplet excitons are harvested through upconversion by *E*-type delayed fluorescence in materials with small singlet–triplet energy gap ΔE_{ST}, based on donor–acceptor (DA) chromophores. Furthermore, organic solar cells (OSCs) might profit from such materials in order to reduce recombination losses. However, targeted design rules for such materials are missing up to now. In this paper, we follow a facile (TD-)DFT-based computational design concept by engineering the fragment frontier orbitals in DA systems. The calculations show that optimized systems with very small ΔE_{ST} in the range of kT can be achieved by balancing the energetic offset between fragment MOs as well as through the nature of the DA connector. Application in OLED will additionally require small non-radiative rates, which recommends large bandgap materials. Utilization in polymeric DA systems with small ΔE_{ST} in OSCs requires the full exploration of the chain length dependence of the respective oligomers.

1. Introduction

The increasing need for cheap, flexible, eco-friendly and sustainable lighting systems has certainly pushed the research in organic light emitting diodes (OLEDs). However, for market success, external quantum efficiencies (EQE) have to be sufficiently high. The most detrimental factors for OLED EQEs are low light outcoupling due to refractive index mismatch at the organic/inorganic interface as well as spin statistics, which generates only 25% singlet states in the emitting layer upon charge recombination [1]. One strategy to overcome the latter problem is the use of triplet emitters, in particular iridium complexes [2]. However, the use of iridium as the least abundant non-radioactive element in the earth's crust might be not the most evident solution to the world's hunger for large-area lighting applications. Recent suggestions are thus aiming at all-organic singlet emitters, which circumvent the problem of spin statistics [3,4]. The general strategy is the generation of an excited state with a small energy difference ΔE_{ST} between the first excited singlet (S_1) and triplet (T_1) states, so that the singlet state can be easily repopulated by triplet upconversion through thermal population. By this so-called *E*-type delayed fluorescence (named after eosin dye, for which it was first observed) [5], the limit of spin statistics can be overcome, thus systems with ΔE_{ST} close to zero are highly desirable materials for OLED development. Moreover, the search for novel host materials for OLEDs with high-lying triplets might also profit from molecules with small singlet–triplet gaps in organic materials [6]. Finally materials with low ΔE_{ST} values might be highly beneficial in organic solar cells to reduce recombination losses [7], as well as for improved materials in spintronics [8] and lasing [9] applications.

One strategy to decrease the singlet–triplet splitting is to increase the chromophore size [10], however, ΔE_{ST} resides usually at about 0.55–0.75 eV at the polymer limit [11]. On the other hand, ΔE_{ST} can be reduced through a donor–acceptor (DA) approach by spatial separation of the

* Corresponding author.
E-mail address: johannes.gierschner@imdea.org (J. Gierschner).

1566-1199/$ - see front matter © 2012 Elsevier B.V. All rights reserved.
doi:10.1016/j.orgel.2012.02.010

highest occupied and lowest unoccupied molecular orbitals (HOMO, LUMO) [12], where the spin exchange interaction is a function of the D–A distance [13]. Spatial separation of the frontier MOs can be achieved in a single molecule, as discussed early on for azulene [14], or in an intermolecular strategy through charge transfer states at the interface of donor and acceptor materials [15]. Intramolecular strategies were recently followed to increase the T_1 energy [16,17] and in consequence to lower ΔE_{ST} [18–20], through appropriate DA materials with pronounced intramolecular charge-transfer (ICT) character of the lowest excited state, thus minimizing ΔE_{ST}.

Novel single molecule materials included metal–organic complexes [3,4,21] and all-organic compounds [18–20], where small ΔE_{ST} were demonstrated by combined fluorescence and phosphorescence studies; repopulation of the singlet state was shown to be operative from delayed fluorescence. However, material design lacks strategic guidelines: for instance, geometrical factors were suggested to be responsible for the spatial separation of the frontier MOs [19,20], but defined rules on how to tune ΔE_{ST}, and at the same time the absolute energetic position of the excited states and thus the emission color were not yet explored. Moreover, the precise nature of the singlet and triplet states was not investigated, instead theoretical descriptions were limited to orbital pictures [4,19]. Last not least, the impact of the ICT character on the S_1 deactivation pathways, and thus on the luminescence efficiency, was not addressed. Therefore, in the following, we undertake a computational approach, based on (time-dependent) density functional theory, (TD-)DFT, to explore these issues in a number of compounds where we systematically vary the chemical structure to separate the parameters which influence the singlet–triplet gap in organic compounds. In doing so, we provide a practical guide for future material design.

2. Results and discussion

The exchange energy, i.e., half the ΔE_{ST} splitting, shows an exponential distance dependence on the respective wave functions [2,11]. Thus, in order to minimize ΔE_{ST}, the occupied and unoccupied MOs which form the respective electronic transition should be spatially separated in different parts of the molecules [12]. In other words, the ICT character of the $S_0 \rightarrow S_1$ transition has to be maximized. In a simple MO correlation picture, such molecules consist of a donor (D) and acceptor (A) fragment where both HOMO and LUMO of D show a positive energetic offset (ΔE_H, ΔE_L) with respect to those of A, so that the S_1 state is described by a promotion of an electron from the HOMO of D to the LUMO of A, see Type II in Fig. 1. However, this can only be realized if the electronic communication between the HOMOs and LUMOs of D and A is well balanced. One limiting case is that no communication is observed and the excitation is localized in one fragment, e.g., described by an excitation $HOMO_A \rightarrow LUMO_A$ (Type I). This will be the case, if the spatial separation between D and A is very large. The other limiting case is the formation of a common HOMO and LUMO, with concomitantly

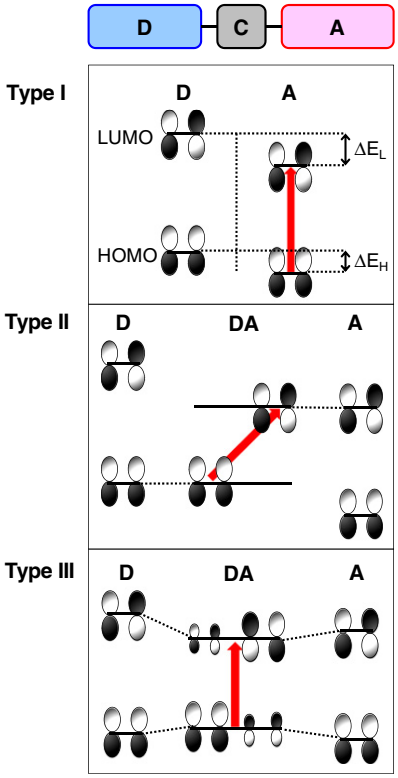

Fig. 1. Schematic orbital representation of different donor–acceptor (D–C–A, C = connector) compounds. Arrows represent electronic excitations in a one-electron approximation.

large orbital delocalization and small ICT character (Type III). The communication between the fragments can be influenced by (i) the amount of the energetic offset ΔE_H, ΔE_L, (ii) the symmetry of the frontier orbitals, (iii) geometrical demands (large dihedral angles), and (iv) the type of connector between the D and A fragments. For these connectors, a hierarchy of increasing communication can be formulated, going from long via short saturated hydrocarbon bridges to connectors with free electron pairs. Within the latter, the connectors might either introduce nodal planes by e.g., *meta*-linkages or promote bond-alternating π-conjugation, e.g., by *para*-/*ortho*-linkages. In order to investigate all these parameters in a systematic way, we picked the structural motif recently presented in an experimental work by Adachi and co-workers, who combined *para*-terphenyl (**3P**)-based units with carbazole (**CZ**)-based units [19].

In a (TD-)DFT based quantum-chemical approach [22], we systematically varied position and type of D and A fragments as well as the connectors outlined above, thus exploring *inter alia* compounds which were not systematically investigated yet neither at an experimental nor at a computational level. TD-DFT calculations based on the standard B3LYP functional give a reasonable description for singlet as well as triplet states of medium-sized molecules [23], including **3P**, **CZ** and fluorene [24], relevant as building blocks for our present work. TD-DFT calculations of ICT states are still a matter of controversy, debating

standard vs. range-separated functionals with results depending strongly on the systems [25,26]. As we will see later, the standard B3LYP functional correctly predicts strongly localized frontier MOs for the D–A compounds under study; thus, they do not suffer from the shortcomings in such cases, in which standard functionals tend to delocalize the MOs and therefore have to be replaced by long-range separated (LRS) functionals. Nevertheless, we further compared the standard B3LYP functional with the LRS exchange–correlation functional CAM-B3LYP for selected molecules. It will be shown later that for all D–A compounds where experimental data are available (compounds **6**, **7**, **8**), B3LYP gives reasonable estimations for both the T_1 and S_1 positions, while CAM-B3LYP makes incorrect estimates of ΔE_{ST} as similarly observed for other long-range corrected functionals [27].

2.1. Role of the substituent position

Compound **1** in Fig. 2 connects the parent **3P** acceptor unit in the *para*-position with the **CZ** donor in the 2-position. The energetic offset between **3P** and **CZ**, $\Delta E_H = 0.36$ eV and $\Delta E_L = 0.30$ eV (Fig. 2), is small enough that common frontier MOs are formed through extension of the π-system, which is delocalized over both fragments (Type III). Due to symmetry reasons, the HOMO of 1 is not formed from the HOMO of **CZ**, but from HOMO − 1. Some asymmetry in the frontier MOs is evident from the orbital pictures (Fig. 2), showing slightly higher LCAO coefficients in the **CZ** part of the HOMO and in the **3P** part of the LUMO.

However, the ICT character of the S_1 state in **1**, formed largely from HOMO → LUMO, is rather small; concomitantly the oscillator strength is considerable large ($f = 1.22$, Table 1). The lowest triplet state T_1 exhibits a similar configuration interaction (CI) description to S_1; it is much lower in energy, resulting in $\Delta E_{ST} = 0.95$ eV, see Fig. 3. In general, orbital localizations in that type of D–π–A systems are possible, however only if the orbital offset ΔE_H, ΔE_L of HOMO and/or LUMOs are large enough to break the electronic communication between A and D. A recent report on substituted oligophenyleneethynylenes demonstrated that the limit of ΔE_H (or ΔE_L) to form a common frontier orbital from molecular fragments in these alternating systems lies somewhat between 1.5 and 2.0 eV [28], thus requiring strong electron withdrawing (donating) groups as substituents in the acceptor (donor) molecular fragments to achieve large MO offsets.

Changing the connection of **CZ** from the 2- to the 9-position (compound **2**), the energy of the frontier MOs is not very different to **1**, however with a very different topology. The HOMO localizes more strongly in the **CZ** moiety and is formed from the HOMO of both fragments. The LUMO is almost entirely localized in the **3P** unity, which is mainly an effect of the dihedral angle of 59° between **3P** and **CZ**; consequently the triplet–singlet gap is reduced to $\Delta E_{ST} = 0.61$ eV, see Fig. 3.

Changing the *para*- to the *meta*-position in **3P** (compound **3**), the conjugation is interrupted [29], so that the fragments cannot form common frontier orbitals. Instead, the HOMO is formed from that of **CZ** and some LCAO contributions in the adjacent phenyl ring, whose symmetry is determined by the **CZ** fragment, see Fig. 2. The LUMO is exclusively localized in the **3P** unit, so that the overlap between the frontier MOs in **3** becomes small, and the S_1 state which is formed mainly from the HOMO → LUMO excitation, shows strong ICT character with small oscillator

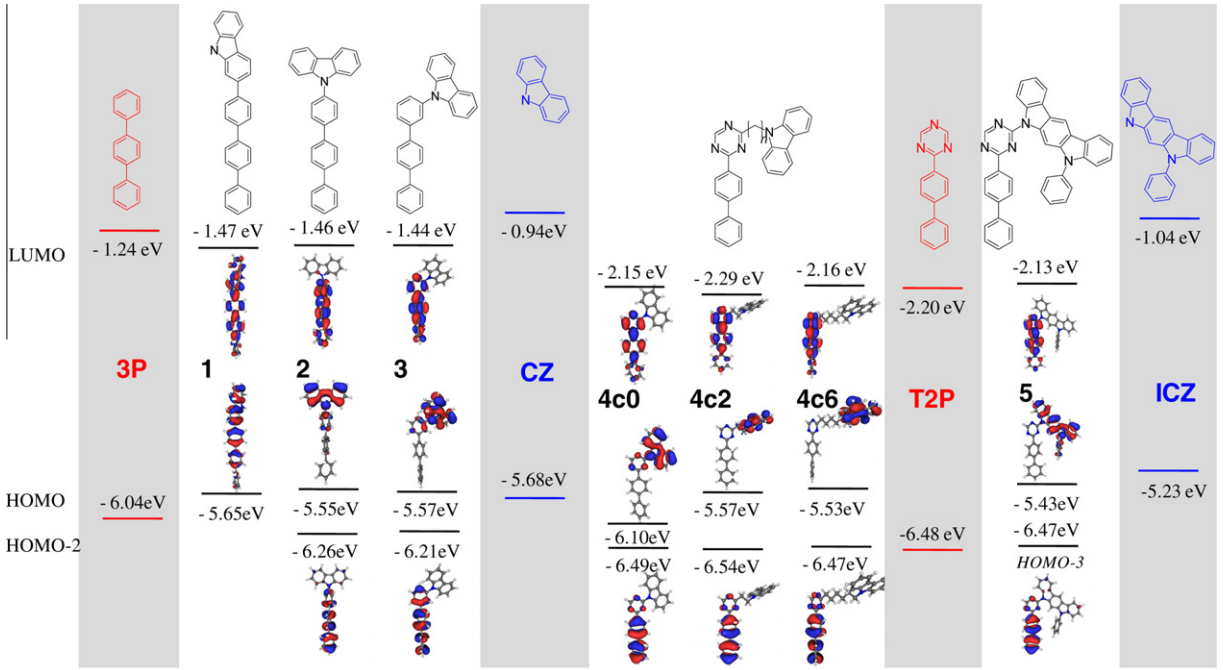

Fig. 2. Calculated frontier orbitals (energies and topologies) of different DA compounds built from fragment MOs (**3P**/**CZ**, **T2P**/**CZ**, and **T2P**/**ICZ**).

Table 1
Fist excited triplet (T_1) and singlet (S_1) states (vertical transition energies) and singlet–triplet gaps ΔE_{ST} of the compounds under study as calculated at the TD-DFT level of theory (B3LYP/6-311G*). Singlet oscillator strength $f(S_1)$ are given in parenthesis. Configuration interaction (CI) is given for relative weights >10%.

		E_{vert} (eV)	CI description	ΔE_{ST} (eV)
3P	T_1	3.10	H → L (79%)	
	S_1	4.42 (0.7020)	H → L (99%)	1.32
T2P	T_1	2.86	H → L (81%)	
	S_1	3.94 (0.7079)	H → L (96%)	1.08
1	T_1	2.82	H → L (74%)	
	S_1	3.77 (1.2231)	H → L (81%) H-1 → L (14%)	0.95
2	T_1	2.99	H-2 → L (44%) H → L (37%)	
	S_1	3.60 (0.3261)	H → L (97%)	0.61
3	T_1	3.07	H-2 → L (74%)	
	S_1	3.64 (0.0111)	H → L (97%)	0.57
4c0	T_1	2.91	H-2 → L (78%)	
	S_1	3.40 (0.0330)	H → L (98%)	0.49
4c2	T_1	2.85	H-2 → L (80%)	
	S_1	2.88 (0.0000)	H → L (100%)	0.03
4c6	T_1	2.87	H-2 → L (80%)	
	S_1	3.13 (0.0000)	H → L (100%)	0.26
5	T_1	2.80	H → L (81%)	
	S_1	2.85 (0.0030)	H → L (99%)	0.05
6	T_1	2.79	H → L (74%)H-2 → L (14%)	
	S_1	2.86 (0.0004)	H → L (99%)	0.07
7	T_1	2.14	H → L (99%)	
	S_1	2.14 (0.0000)	H → L (100%)	0.004
8	T_1	2.74	H → L + 1 (68%)	
	S_1	3.33 (0.545)	H → L + 1 (98%)	0.59
	S_2	3.36 (0.0022)	H → L (99%)	

strength, see Table 1. The T_1 state, situated 0.57 eV below S_1, is now largely described by a HOMO − 2 → LUMO excitation (Table 1), where both orbitals are localized on the **3P** unit, see Fig. 2; accordingly, the triplet energy is very similar to that of free **3P**, see Table 1.

2.2. Role of the acceptor fragment

Substituting the terminal phenyl ring of **3P** by 1,3,5-triazine (**T2P**) in compound **4c0** leads to substantial lowering of the frontier MOs due to the lower lying orbitals of **T2P** (Fig. 2), thus enlarging the orbital offsets to ΔE_H = 0.80 eV and ΔE_L = 1.26 eV, while the dihedral angle at the **CZ** unit in **4c0** (22°) is much smaller compared to **3** (60°). The singlet–triplet gap energy of **4c0** reduces to ΔE_{ST} = 0.49 eV, somewhat lower compared to **3**, demonstrating the primacy of the energy gain in the orbital offsets, which reduces communication between the frontier MOs, against the planarization effect, which enhances communication.

2.3. Role of the DA connector

The separation between the D and A fragments was enlarged by introducing a saturated $(CH_2)_n$ linker to decrease the electronic communication. In fact, for n = 2 (**4c2**), both HOMO and LUMO become completely separated (Fig. 2), the S_1 oscillator strength reduces to zero ($f = 2 \times 10^{-6}$) and the singlet–triplet energy difference drops sharply to ΔE_{ST} = 0.03 eV for the vertical singlet–triplet gap (in vacuum), thus at first sight providing an interesting structural motif for triplet upconversion. Solvent inclusion yields a somewhat larger gap (0.15 eV). In any case, the probability for triplet upconversion will depend on the *adiabatic* singlet–triplet gap $\Delta E_{ST,0}$, i.e., the energy difference between the minima of the potential hypersurface. Excited state optimization of S_1 and T_1 in vacuum yields $\Delta E_{ST,0}$ = 0.19 eV (see Table 2), due to a stronger geometry relaxation in T_1 (0.46 eV) compared to S_1 (0.30 eV), as induced by stronger excited state planarization in T_1.

Since the overlap between the wave functions in **4c2** is already minimized, further reduction of the electronic communication by increasing n does not further decrease ΔE_{ST} but increases it due to the increased spatial

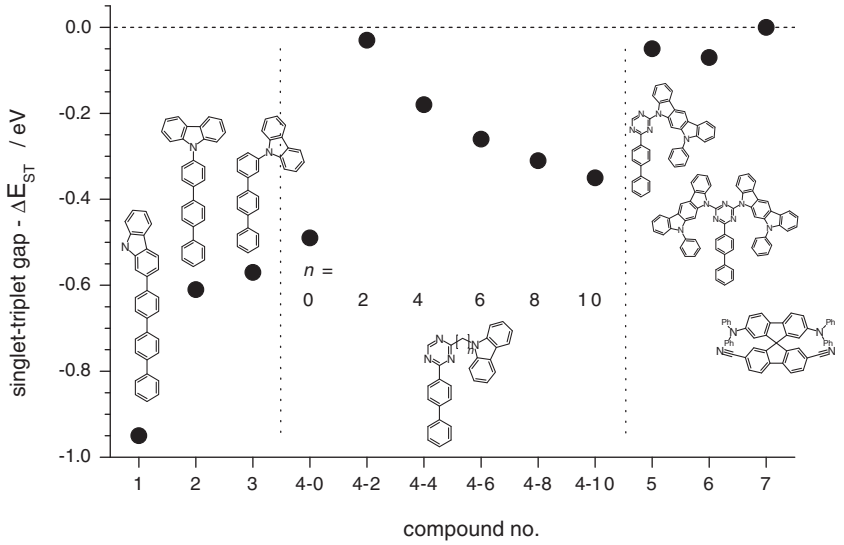

Fig. 3. Calculated singlet–triplet gaps ΔE_{ST} for DA compounds.

Table 2
Calculated (B3LYP) results for vertical (E_{vert}) and adiabatic (E_{adiab}) transition energies, reorganization energies ($\Delta E_{re} = E_{vert} - E_{adiab}$) and singlet triplet gaps (ΔE_{ST}) for compounds with small S–T gap (in vacuo; in eV).

		E_{vert}	E_{adiab}	ΔE_{re}
4c2	T_1	2.85	2.39	0.46
	S_1	2.88	2.58	0.30
	ΔE_{ST}	0.03	0.19	
5	T_1	2.80	2.30	0.50
	S_1	2.85	2.32	0.53
	ΔE_{ST}	0.05	0.02	
6	T_1	2.79	2.40	0.39
	S_1	2.86	2.44	0.42
	ΔE_{ST}	0.07	0.04	
7	T_1	2.14	1.87	0.27
	S_1	2.14	1.89	0.25
	ΔE_{ST}	0.004	0.02	

separation of the MOs, slowly approaching the Type I limit, see Fig. 3.

2.4. Role of the donor fragment

In a last step we optimized the donor fragment, substituting the carbazole donor unit in **4c0** by indolo[2,3-a]carbazole (**ICZ**), forming compound **5**, leads to a substantial decrease of the vertical singlet–triplet gap to ΔE_{ST} = 0.05 eV (Fig. 3); the adiabatic gap is $\Delta E_{ST,0}$ = 0.02 eV. The decrease of the gap is primarily due to the increase of the HOMO energy of the donor compared to **CZ**, see Fig. 2, which increases the energetic offset between the fragment HOMO levels ΔE_H from 0.8 eV to 1.25 eV, and thus substantially decreases the electronic communication between the fragments' HOMOs as can be seen in the topology, see Fig. 2. Bis-**ICZ**-substituted **T2P** (**6**, see Fig. 3) was recently synthesized by Adachi and co-workers [19]. Our calculated vertical singlet transition $E_{vert}(S_1)$ = 2.86 eV for 6 (Table 1) compares reasonably well with the expected S_1 absorption maximum from experiment in solution, $E_{max} \approx 3.00$ eV [31], while the long-range separated functional places the S_1 state 1 eV too high in energy [32]. Inclusion of solvent in the TD-DFT scheme leads to a small hypsochromic shift, now placing the calculated transition at $E_{vert}(S_1)$ = 2.91 eV. The vertical and adiabatic singlet–triplet gaps (Table 2) are calculated to be similarly small as in **5** with ΔE_{ST} = 0.07 eV and $\Delta E_{ST,0}$ = 0.04 eV, see Fig. 3, close to the experimental result of ca. 0.11 eV [19], which was estimated from the onsets of the fluorescence and phosphorescence spectra. Different to compounds **3** and **4cn**, the calculated T_1 state in compounds **5** and **6** (as well as in **7**, *vide infra*) is formed by a HOMO → LUMO transition like S_1 (Table 1), as calculated by the standard as well as by the long-range separated DFT functionals, thus predicting high ICT character for both transitions.

2.5. Towards compounds with zero singlet–triplet splitting

It should be stressed that as in **4c0**, in **6** geometrical factors also play a minor role in the spatial separation of the frontier orbitals: the dihedral angle between the triazine ring and the **ICZ** moiety is only 22°, thus not substantially blocking possible conjugation. Moreover, a single point calculation on the planarized molecule does not change the picture drawn above. Nevertheless, one expects that imposing an essentially perpendicular situation between the fragments should further enhance orbital localization. Most promising in this respect should be spiro-compounds, which were intensively investigated in the past [33]. However, most of the spiro-based molecules reported so far do not show very small singlet–triplet gaps [17], an effect which we attribute to the insufficient orbital offset of the fragment MOs as outlined above. It was only recently that a spiro-compound with very small ΔE_{ST} was reported by Hung et al. [18], where one fluorene fragment is substituted with strong electron acceptors, i.e., cyano-groups, whereas the other fluorene carries diphenylamino-substituents (compound **7**, see Fig. 4). This indeed imposes large orbital offsets of ΔE_H = 2.08 eV and ΔE_L = 1.46 eV and leads to strong localization of the frontier MOs in the spiro compound (Fig. 4) with a vanishing singlet–triplet gap ($\Delta E_{ST} = \Delta E_{ST,0}$ = 0.004 eV), see Table 1. The calculations place the transitions about 0.4 eV below the experimental value, which might be due to the rather large size of the conjugated system in **7**, where DFT-based methods generally underestimate the experimental transition energies [34,35]. In any case, the experimental results qualitatively confirm our calculations, showing a very small energy difference of the PH and FL spectral origins [18]. Moreover, the experimentally observed large apparent Stokes-shift between the main absorption ($E_{max,exp}$ = 3.24 eV) and FL (2.23 eV) is attributed to the strong ICT character of the $S_0 \rightarrow S_1$ transition with vanishing oscillator strength (Table 1); the main absorption is assigned to the first strong singlet transition (S_5, 3.40 eV).

Nevertheless, proper engineering not only of the frontier MOs, but also of the next higher (lower) lying orbital (LUMO + 1, HOMO − 1) is crucial to generate small singlet triplet gaps. A striking example is the spiro-compound 8 [36], see Fig. 4. Here, LUMO and LUMO + 1 are very close in energy, so that correlation becomes very important. Although the HOMO and LUMO are exclusively localized on the donor and acceptor parts, respectively, the calculations predict a large singlet triplet gap (ΔE_{ST} = 0.59 eV, Table 1) due to the low-lying LUMO + 1 orbital, which induces a complex CI description. Also here, the B3LYP prediction of the singlet triplet gap and a high oscillator strength for S_1 (Table 1) agree well with experiment, from which the gap can be estimated to $\Delta E_{ST} \approx 0.5$ eV [36].

3. Conclusion and outlook

In conclusion, we have explored a simple computational design concept for materials with small singlet–triplet gap and tunable emission color by engineering the fragment frontier orbitals. The singlet–triplet gap ΔE_{ST} depends sensitively on the extent of the spatial separation of the HOMO and LUMO in the donor (D) and acceptor (A) parts of the molecules [13]; already small MO overlap leads to a significant widening of ΔE_{ST}. Orbital localization is mainly driven by the energy offset of the respective MOs for the D

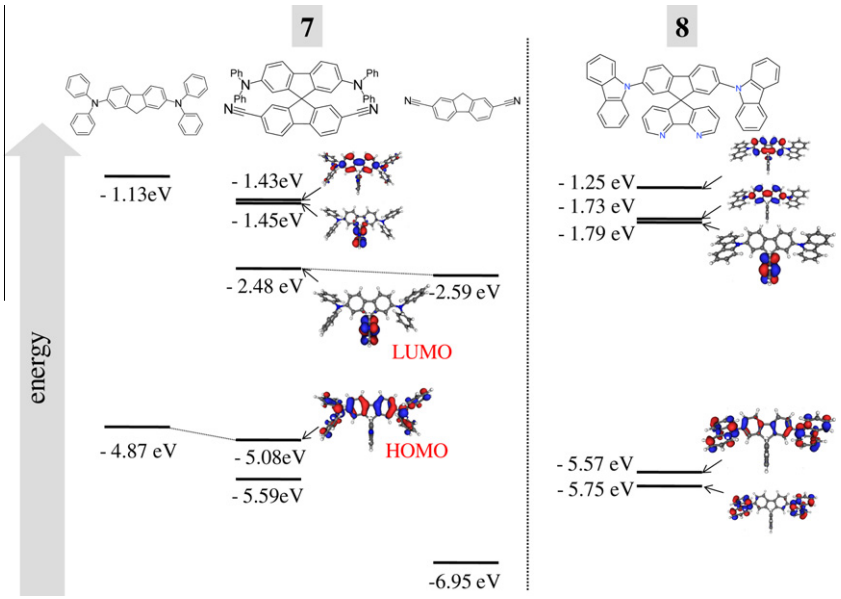

Fig. 4. Frontier MOs for compound **7** (with fragment MOs) and compound **8**.

and A fragments, but only to a smaller part by geometrical factors. In any case, a perpendicular situation for the frontier MOs through twisted structures as well as a balanced distance between the D and A moieties through a saturated spacer significantly assists the reduction of ΔE_{ST}. Proper MO design also requires the energetic separation of HOMO − 1 and LUMO + 1 from the frontier MOs, to avoid widening of ΔE_{ST} due to configuration interaction. The sterically demanding architecture utilized by Adachi et al. in **6** and Hung et al. in **7** additionally ensures minimized intermolecular interactions in the solid state; such interactions are expected to significantly influence excited state energies [30], and thus – depending on their type and strength – possibly oppose the design strategy.

For the small singlet–triplet gap a price has to be paid: zero gap means negligible MO overlap and thus zero oscillator strength $f(S_1)$. Although in real experiments, environmental inhomogeneities as well as coupling to higher states will lead to non-vanishing f, the resulting rate constant of fluorescence (which is directly proportional to f) will be anyway small. Thus, fluorescence quantum yields Φ_F might be small as well if non-radiative deactivation pathways via internal conversion (IC) processes are efficient. Recent experimental results give hope: for compound **6**, $\Phi_F = 39\%$ (10% prompt and 29% delayed) was reported [19], indicating rather moderate non-radiative rate constants. This might be mainly due to the rather large optical gap of compound **6**, [19], thus making molecules with small singlet–triplet gaps and large optical gap indeed interesting compounds for OLED applications.

Poly-conjugated materials with small singlet–triplet gaps might also attract considerable interest in organic solar cells to reduce recombination losses [7]. The DA strategy for low bandgap polymers, which is frequently followed to efficiently harvest sunlight [37], could thus have additional virtue. Localization of the frontier MOs in DA polymers is however an intricate issue: fragment MO considerations for small oligomers as representatives of the polymers are not sufficient to understand the behavior at the polymer limit, since the energetic positions of localized and delocalized MOs might cross at a certain chain length [28]; therefore the evolution with chain length has to be carefully analyzed [28,34,38].

Acknowledgments

The work was supported by the Spanish 'Ministerio de Economia y Competitividad' (MEC, Project ConMol, Grant No. CTQ2011-27317) and the Comunidad Madrid (project NanoBioMagnet, Grant No. S2009/MAT-1726). We thank E. Ortí for access to the computing facilities of the group at the University of Valencia. J.G. is a Ramón y Cajal research fellow of the MEC.

Appendix A. Supplementary data

Supplementary data associated with this article can be found, in the online version, at doi:10.1016/j.orgel.2012.02.010.

References

[1] C. Adachi, M.A. Baldo, S.R. Forrest, M.E. Thompson, J. Appl. Phys. 11 (1999) 285.
[2] H. Yersin (Ed.), Highly Efficient OLEDs with Phosphorescent Materials, Wiley-VCH, Weinheim, 2008.
[3] A. Endo, M. Ogasawara, A. Takahashi, D. Yokoyama, Y. Kato, C. Adachi, Adv. Mater. 21 (2009) 4802.
[4] J.C. Deaton, S.C. Switalski, D.Y. Kondakov, R.H. Young, T.D. Pawlik, D.J. Giesen, S.B. Harkins, A.J.M. Miller, S.F. Mickenberg, J.C. Peters, J. Am. Chem. Soc. 132 (2010) 9499.
[5] J. Guillet, Polymer Photophysics and Photochemistry – An Introduction to the Study of Photoprocesses in Macromolecules, Cambridge University Press, England, 1987.

[6] For a recent review see H. Sasabe, J. Kido, Chem. Mater. 23 (2011) 621.
[7] D. Veldman, S.C.J. Meskers, R.A.J. Janssen, Adv. Funct. Mater. 19 (2009) 1939.
[8] (a) V.A. Dediu, L.E. Hueso, I. Bergenti, C. Taliani, Nat. Mater. 8 (2009) 707;
(b) T.D. Nguyen, G. Hukic-Markosian, F. Wang, L. Wojcik, X.-G. Li, E. Ehrenfreund, Z.V. Vardeny, Nat. Mater. 9 (2010) 345.
[9] [a] N.C. Giebink, S.R. Forrest, Phys. Rev. B 79 (2009) 073302;
[b] J.M. Lupton, Nature 453 (2008) 459.
[10] [a] G.D. Scholes, G. Rumbles, Nat. Mater. 5 (2006) 683;
[b] G.D. Scholes, ACS Nano 2 (2008) 523.
[11] [a] A. Köhler, H. Bässler, Mater. Sci. Eng. R66 (2009) 71;
[b] A. Köhler, D. Beljonne, Adv. Funct. Mater. 14 (2004) 11.
[12] M. Klessinger, J. Michl, Excited States and Photochemistry of Organic Molecules, VCH, Weinheim, 1995.
[13] H.-G. Busmann, H. Staerk, A. Weller, J. Chem. Phys. 91 (1989) 4098.
[14] J. Michl, E.W. Thulstrup, Tetrahedron 32 (1976) 205.
[15] S. Difley, D. Beljonne, T. Van Voorhis, J. Am. Chem. Soc. 130 (2008) 3420.
[16] K. Brunner, A. van Dijken, H. Börner, J.J.A.M. Bastiaansen, N.M.M. Kiggen, B.M.W. Langeveld, J. Am. Chem. Soc. 126 (2004) 6035.
[17] I. Avilov, P. Marsal, J.-L. Brédas, D. Beljonne, Adv. Mater. 16 (2004) 1624.
[18] W.-Y. Hung, T.-C. Tsai, S.-Y. Ku, L.-C. Chi, K.-T. Wong, Phys. Chem. Chem. Phys. 10 (2008) 5822.
[19] A. Endo, K. Sato, K. Yoshimura, T. Kai, A. Kawada, H. Miyazaki, C. Adachi, Appl. Phys. Lett. 98 (2011) 083302.
[20] D. Chaudhuri, H. Wettach, K.J. van Schooten, S. Liu, E. Sigmund, S. Höger, J.M. Lupton, Angew. Chem. Int. Ed. 49 (2010) 7714.
[21] S. Haneder, E. Da Como, J. Feldmann, J.M. Lupton, C. Lennartz, P. Erk, E. Fuchs, O. Molt, I. Münster, C. Schildknecht, G. Wagenblast, Adv. Mater. 20 (2008) 3325.
[22] Geometries, MO energies and topologies were calculated at the DFT level using the B3LYP (as well as the long-range separated exchange–correlation functionals CAM-B3LYP and LC-ωPBE) functional and the 6-311G* basis set, as implemented in the Gaussian03 program package, see Ref. [39]. Due to considerable sterical demands of the compounds, optimizations were performed without imposing planarity. Instead, for molecules with symmetrical donor substitution (2, 6, 7), we chose the C_2 point group. This inhibits MO localization in one donor branch. DFT calculations were carried out in vacuo, TD-DFT calculations of the vertical transition energies were alternatively done also in solvent (dichloromethane), using the PCM model (standard parameters). Adiabatic transition energies were calculated within the Turbomole package, see Ref. [40]. Orbital topologies were plotted with Molekel, Ref. [41].
[23] [a] M. Parac, S. Grimme, Chem. Phys. 292 (2003) 11;
[b] K.A. Nguyen, J. Kennel, R. Pachter, J. Chem. Phys. 117 (2002) 7128.
[24] X. Liu, D. Yang, H. Ju, F. Teng, Y. Hou, Z. Lou, Chem. Phys. Lett. 503 (2011) 75.
[25] D. Jacquemin, E.A. Perpete, I. Ciofini, C. Adamo, Acc. Chem. Res. 42 (2009) 326.
[26] D. Casanova, F.P. Rotzinger, M. Grätzel, J. Chem. Theory Comput. 6 (2010) 1219.
[27] J.S. Sears, T. Koerzdoerfer, C.-R. Zhang, J.-L. Brédas, J. Chem. Phys. 135 (2011) 151103.
[28] T. Dutta, K.B. Woody, S.R. Parkin, M.D. Watson, J. Gierschner, J. Am. Chem. Soc. 132 (2009) 17321.
[29] L. Pascal, J.J. Vanden Eynde, Y. Van Haverbeke, P. Dubois, A. Michel, U. Rant, E. Zojer, G. Leising, L.O. Van Dorn, N.E. Gruhn, J. Cornil, J.L. Brédas, J. Phys. Chem. B 106 (2002) 6442.
[30] [a] J. Gierschner, M. Ehni, H.-J. Egelhaaf, B. Milián Medina, D. Beljonne, H. Benmansour, G.C. Bazan, J. Chem. Phys. 123 (2005) 144914;
[b] J. Gierschner, H.-G. Mack, D. Oelkrug, I. Waldner, H. Rau, J. Phys. Chem. A 108 (2004) 257.
[31] The S_1 state is not visible in the experimental absorption spectrum due to the low oscillator strength, but the vertical transition energy can be estimated from $E_{vert}(S_0 \rightarrow S_1) = E_{00} + \Delta E$, ie. from the adiabatic transition E00 and the reorganization energy ΔE. While the former is estimated from half height in the rising edge of the FL spectrum (E_{00} = 2.76 eV), the latter is obtained from $\Delta E = E_{00} - E_{vert}(S_1 \rightarrow S_0)$, with $E_{vert}(S_1 \rightarrow S_0)$ = 2.52 eV (estimated from the FL maximum) to give $E_{vert}(S_0 \rightarrow S_1)$ = 3.00 eV.
[32] CAM-B3LYP results of the vertical and adiabatic transition energies for compounds **4c2**, **5**, **6**, and **7** are reported in Table S1 the Supplementary content.
[33] For a recent review see T.P.I. Saragi, T. Spehr, A. Siebert, T. Fuhrmann-Lieker, J. Salbeck, Chem. Rev. 107 (2007) 1011.
[34] J. Gierschner, J. Cornil, H.-J. Egelhaaf, Adv. Mater. 19 (2007) 173.
[35] CAM-B3LYP on the other side, largely overestimates the experimental value for ΔE_{ST} of compound **7**, see Table S1.
[36] W.-Y. Hung, T.-C. Wang, H.-C. Chiu, H.-F. Chen, K.-T. Wong, Phys. Chem. Chem. Phys. 12 (2010) 10685.
[37] For a recent review, see e.g. A. Facchetti, Chem. Mater. 23 (2011) 733.
[38] (a) B.P. Karsten, L. Viani, J. Gierschner, J. Cornil, R.A.J. Janssen, J. Phys. Chem. A 113 (2009) 10343;
(b) J. Gierschner, B. Milián-Medina, in preparation.
[39] M.J. Frisch et al., Gaussian, Inc., Wallingford CT, 2003.
[40] Turbomole program 5.8 program package R. Ahlrichs, M. Bär, M. Häser, H. Horn, C. Kölmel, Chem. Phys. Lett. 162 (1989) 165.
[41] P. Flükiger, H. P. Lüthi, S. Portmann, J. Weber, MOLEKEL, Version 4.3; Swiss National Computing Centre CSCS, Manno, Switzerland, 2000, <http://www.cscs.ch/molkel/>.